Purdue University

Purdue e-Pubs

International Refrigeration and Air Conditioning Conference

School of Mechanical Engineering

2022

On the Pressure Drop of Various Hydraulic Pipes Including 90-Degree Bends and T-Shape Manifolds: 1-D and 3-D Analyses

Hyun Jin Kwon

Yeong Jun Yun

Se-Myong Chang

Yong Cho

Follow this and additional works at: https://docs.lib.purdue.edu/iracc

Kwon, Hyun Jin; Yun, Yeong Jun; Chang, Se-Myong; and Cho, Yong, "On the Pressure Drop of Various Hydraulic Pipes Including 90-Degree Bends and T-Shape Manifolds: 1-D and 3-D Analyses" (2022). *International Refrigeration and Air Conditioning Conference.* Paper 2432.
https://docs.lib.purdue.edu/iracc/2432

This document has been made available through Purdue e-Pubs, a service of the Purdue University Libraries. Please contact epubs@purdue.edu for additional information.
Complete proceedings may be acquired in print and on CD-ROM directly from the Ray W. Herrick Laboratories at https://engineering.purdue.edu/Herrick/Events/orderlit.html

On the Pressure Drop of Various Hydraulic Pipes Including 90-Degree Bends and T-Shape Manifolds: 1-D and 3-D Analyses

Hyun Jin KWON[1], Yeong Jun YUN[2], Se-Myong CHANG[3*], Yong CHO[4]

[1]Kunsan National University, Department of Mechanical Engineering,
Jeonbuk, Gunsan-si, Republic of South Korea
kint12@naver.com

[2] Kunsan National University, Department of Mathematics,
Jeonbuk, Gunsan-si, Republic of South Korea
yun-yj@kunsan.ac.kr

[3] Kunsan National University, School of Mechanical Convergence System Engineering,
Jeonbuk, Gunsan-si, Republic of South Korea
smchang@kunsan.ac.kr

[4] K-water Institute, Korea Water Resources Cooperation
Deajoen, Daedeok-gu, Republic of South Korea
ycho@kwater.or.kr

* Corresponding Author

ABSTRACT

In this research, we conducted numerical simulations of 90-degree bend and T-junction between Reynolds numbers 100,000~10,000,000 to get the minor(or dynamic) loss coefficients for the purpose of simplifying the three-dimensional CFD to one-dimensional analysis, branching the main pipe into the branch pipe of tees with parameters of varying area and flow rate ratio. As the ratio of flow rate changes, inflection points are found in the distribution of minor losses in both separated and jetted flow. Finally, a simple one-dimensional problem was solved using a commercial 1-D Solver based on minor losses computed from the results of 3-D Solver, and also verified with the acceptable calculation results.

1. INTRODUCTION

In the fields of many engineering areas, the pipeline systems are installed to transport water from rivers and dams, and, for each destination, the fluid must be stably transported through branch, satisfying the designed flow rate. Most of the branch pipes separated from main pipe are installed in a T-shape branch, and this shape causes the pressure losses because of rapid change of the flow path. The pressure losses are classified into two categories: the major losses that occurs with friction and minor losses originated from components as fittings, valve, bend, etc(White, 2016). Their pressure losses in a piping system is an important factor that hinders transport of fluids, and furthermore, since the geometrical and physical ratio between the main and branch pipe are different for each shape, it is essential to evaluate the data of pressure drop or minor losses. Figure 1 is schematic diagram of dividing flow in a T-shape pipe where the cross-sectional areas A's are defined. To predict the minor losses from flow path, Oka et al, (1996) conducted the experiment with a fixed area ratio, A_2/A_3=17.72, and also Oka and Ito (2005) conducted the experiment with area ratio, A_2/A_3=11.44 and various angles between main and branch pipe. However, it is difficult

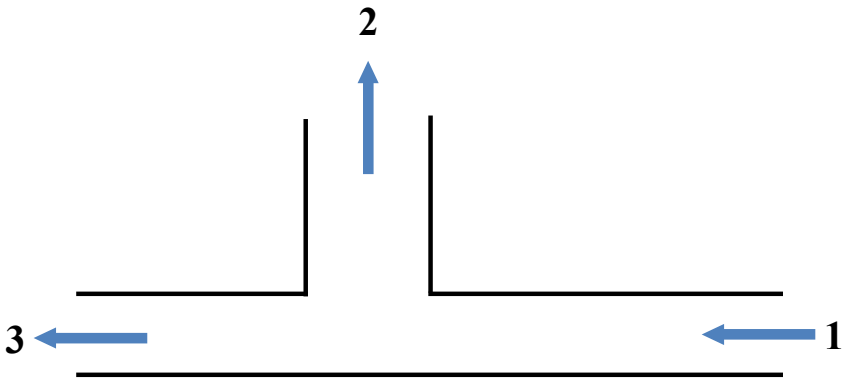

Figure 1: Configuration of flow direction of T-junction

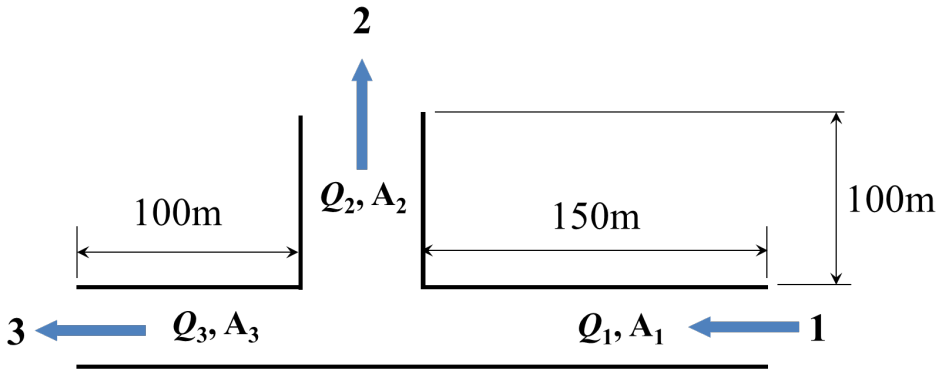

Figure 2: Configuration of present model for dividing flow

to observe the flow characteristics transparently due to unsteadiness in their experimental data. In the last few decades, since not only the performance of computer but also development of commercial code has been increased, many researchers come to be able to predict the flow characteristics and pressure losses, easily(Costa et al, 2006; Badar et al, 2012; Abdulwahhab et al., 2013; Zhang and Wang, 2019). However, as a real pipeline system is intertwined, and also has the very long pipe rather with three-dimensional flow, it takes a lot of simulation time consumed for three-dimensional modeling and generation of the mesh. Therefore, 3-D numerical simulation of a pipe system is limited in the practical duty only for the local zone where flow changes. Recently, quick numerical prediction become possible for the computation of the pressure drop or losses by analyzing pipeline system using the one-dimensional solver with easy extension such as the installation of the additional pump or added flow rate at each point. The reliability of 1-D solution depends on the precision of basic parameters input to the software including minor losses as well as Darcy friction coefficients. Therefore, for the achievement of the acceptable numerical solution, the accurate minor loss must be specified as the input condition.

In this research, we perform the numerical simulations using a commercial code ANSYS-CFX, the Reynolds number based on pipe diameter between 100,000 and 10,000,000 with respect to 90-degree bend and area/flow rate ratio to obtain the chart of minor losses, and also their results is compared with Miller's chart(Miller, 1986) for validation. Finally, a simple non-loop system is simulated using the 1-D solver KYPIPE based on minor losses from results of 3-D solver, ANSYS-CFX.

2. DEFINITION OF NUMERICAL PROBLEM

2.1 Governing Equations

The three-dimensional Navier-Stokes equations for incompressible flow are written as:

$$\nabla \cdot V = 0 \tag{1}$$

$$(V \cdot \nabla)V - = \frac{1}{\rho}\nabla p + \nu\nabla^2 V \tag{2}$$

where, V is velocity vector, ρ is density, p is pressure, and ν is kinematic viscosity, respectively. In this research, since the Reynolds number based on diameter greater than critical Reynolds number, 2,300 in internal flow, we choose the standard k-ε turbulence model, which demonstrated good performance of internal flow for many engineering problems(Versteeg and Malalassekera, 2007).

$$\nabla \cdot (kV) = \nabla \cdot \left(\frac{\nu_t}{\sigma_k}\nabla k\right) + 2\nu_t(S_{ij}S_{ij}) - \varepsilon \tag{3}$$

$$\nabla \cdot (\varepsilon V) = \nabla \cdot \left(\frac{\nu_t}{\sigma_\varepsilon}\nabla \varepsilon\right) + C_{1\varepsilon}\frac{\varepsilon}{k}2\nu_t(S_{ij}S_{ij}) - C_{2\varepsilon}\frac{k}{\varepsilon^2} \tag{4}$$

where, the k and ε equations (3-4) are transport equation of turbulence kinetic energy and turbulence energy dissipation rate, ν_t is kinematic eddy viscosity, and S_{ij} is strain-rate tensor, respectively. The coefficients of standard k-ε turbulence model are presented as Table 1.

Table 1: Standard k-ε model constants

C_μ	σ_k	σ_ε	$C_{1\varepsilon}$	$C_{2\varepsilon}$
0.09	1.00	1.30	1.44	1.92

2.2 Minor Loss

A schematic diagram on dividing or separating flow is shown in Figure 2. With the entrance section denoted by 1, branch denoted by 2, and downstream section denoted by 3. The global energy equation is

$$p_1 + \frac{1}{2}\rho u_1^2 = p_k + \frac{1}{2}\rho u_k^2 + f_1\frac{L_1}{D_1}\frac{1}{2}\rho u_1^2 + f_k\frac{L_k}{D_k}\frac{1}{2}\rho u_k^2 + \Delta p_{1k} \tag{5}$$

where, second and third-term in right hand side defined as Darcy-Weisbach equation, f is Darcy friction factor which is defined as Colebrook-White equation in turbulent flow(Menon, 2015). In this case, when the flow path is described from entrance to branch surface, the minor loss is defined as follows(Zhang and Wang, 2019).

$$K_{12} = \frac{\Delta p_{12} - \left[\frac{1}{2}\rho(u_1^2 - u_2^2)\right]}{\frac{1}{2}\rho u_1^2} \tag{6}$$

2.3 Mesh Information and Boundary Conditions

Figure 3 shows mesh information and boundary conditions. The total number of mesh in bend pipe is about 4.4 M(million); the inflow boundary conditions applied as a fully-developed velocity profile; and a sufficiently long length was given as buffer zones to reduce the numerical instability by effect of the bend in the inlet and outlets. The mesh information is shown in Figure 4, where the element size of tetrahedral type defined as 0.15M, and the number of mesh is about 5 to 6.5M, depending on the area ratio. The boundary conditions is shown in Table 2. Finally, a first layer thickness of prism layer for all of the numerical cases was defined based on y^+ =30 to which the wall function is applicable.

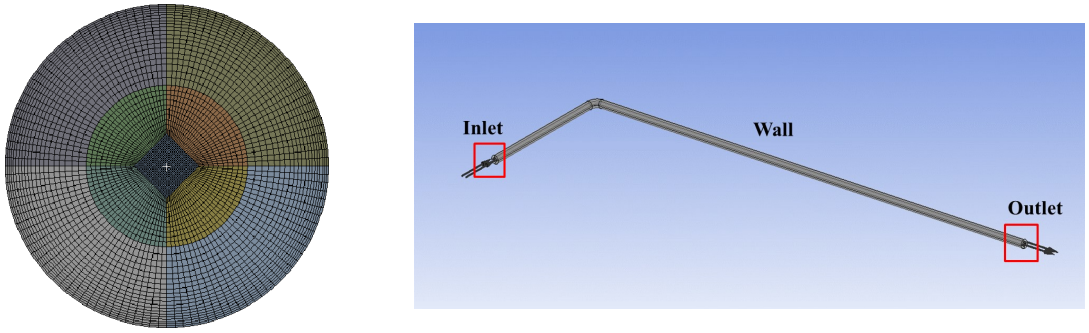

(a) **(b)**

Figure 3: Bend pipe: (a) Surface mesh at inflow boundary, (b) Boundary conditions

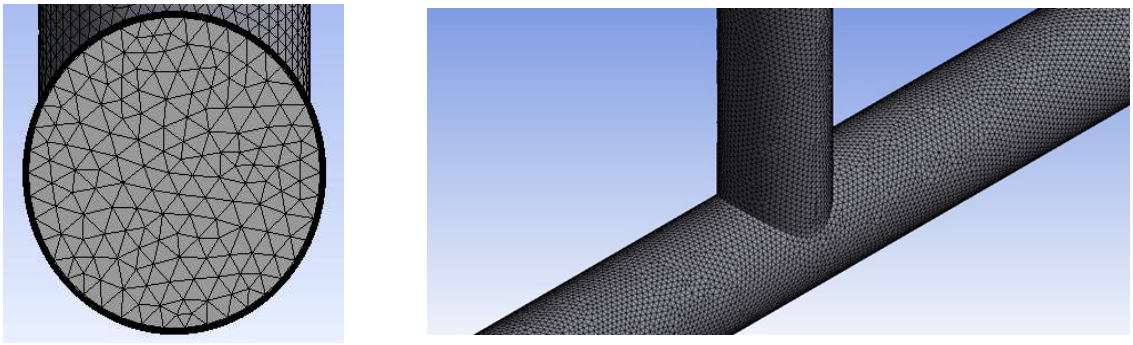

(a) **(b)**

Figure 4: Mesh Configuration of T-junction: (a) Surface mesh at inflow boundary, (b) Zoomed view

Table 2: Boundary conditions of T-junction model

Location		**Value**			
Upstream		Static gauge pressure = 0 [Pa]			
Branch	Flow rate ratio	0.2	0.4	0.6	0.8
Downstream	(Q_k/Q_1)	0.8	0.6	0.4	0.2

3. RESULT AND DISCUSSION

3.1 Validation: Bend Pipe

For the bend pipe problem presented in Figure 3, the head losses were calculated at the four positions as shown in Figure 5 to validate the code. Figure 6 is plotting the head losses and minor loss coefficients. Figure 6(a) compares the distribution of head loss for each quarter point of circle (such as top, bottom, inner-side, and outer-side), shown as a reasonable result. In Figure 6(b), the effect of centrifugal force in the rotation of bended flow results in decrease or increase of the head losses at inner and outer sides, respectively. However, in figure 6(b), the present results predict under-estimation from the empirical correlation of Ito (1960) because on the other hand, this numerical simulation uses ideal smooth wall, so additional losses occurred by wall roughness are not considered. Many other

references (Csizmadia and Hos, 2014; Ayala and Cimbala, 2020) also have shown the similar result that the numerical simulation predicts the minor loss less than that of experiment.

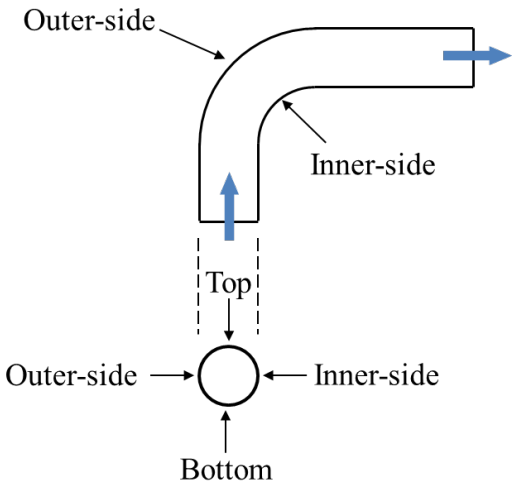

Figure 5: Probe location of bend pipe

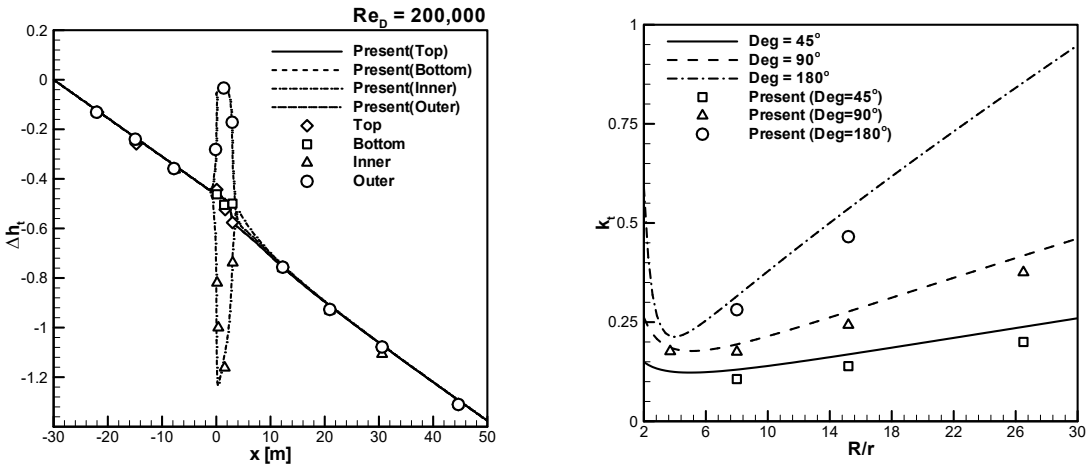

(a) (b)

Figure 6: Comparison of the present and reference(Ito, 1960) for bend pipe:
(a) Head losses, (b) Minor loss coefficients.

3.2 Validation: T-Junction

Figure 7 is the plot of minor losses which is compared with the present and references(Gardel, 1957; Boldy 1970; Ito and Imai, 1973; Miller, 1986; Maia, 1992; Costa et al, 2006). Gardel(1967)'s result predicted the underestimation compared to other references because that study used a T-shape pipe filleted at branch which is reducing the pressure losses. As the flow rate ratio increases, the tendency of minor losses coefficients reduces, and then increases due to the size of separation bubble as shown in Figure 9. Therefore, as the flow rate ratio increases, the size of the separation bubble shrinks, which results in a jet flow because of reduction of the flow rate in branch pipe and increase of the velocity magnitude behind the branch pipe from the continuity law. Although this jet flow plays a role in reducing the minor losses by shrinking the size of the separation bubble, as the flow rate ratio increases, the

flow path to the branch pipe is rapidly changed, which causes the minor losses to increase. This present result has shown acceptable minor losses compared with references, and validated.

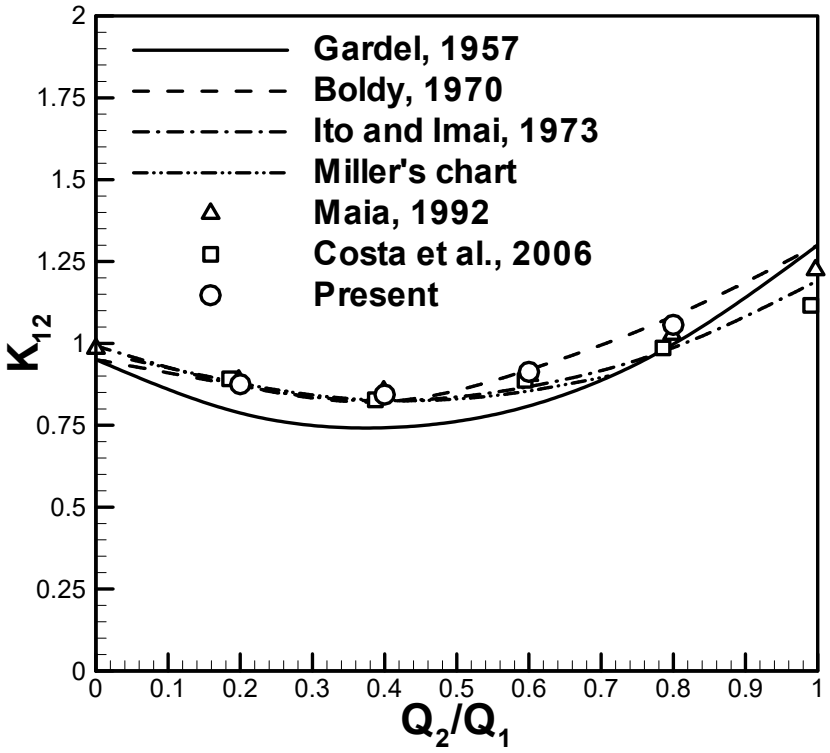

Figure 7: Numerical validation of minor loss coefficients for flow of the upstream into the branch pipe of tees at A_2/A_1=1.0

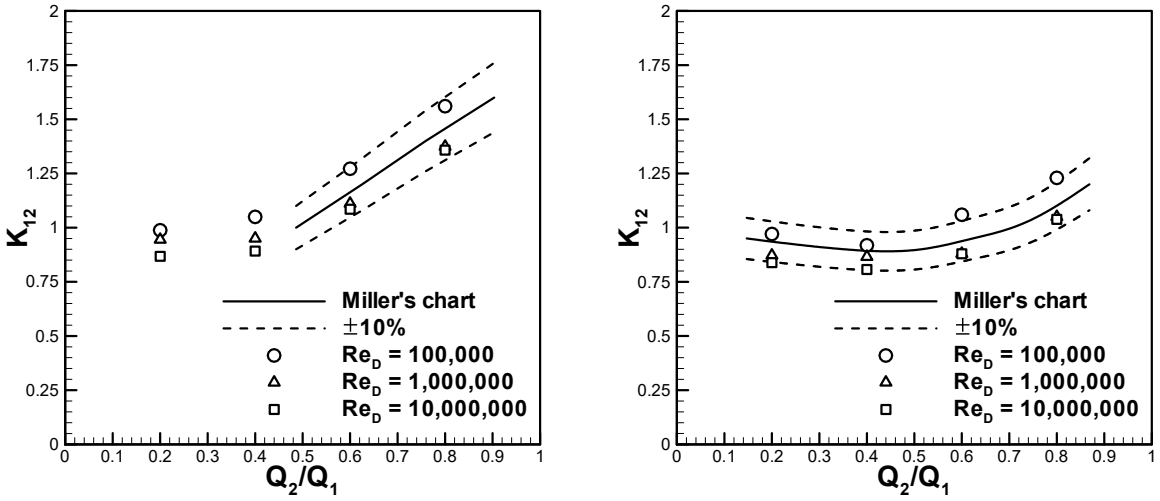

(a) (b)

Figure 8: Comparison of the minor losses coefficients for flow of the upstream into the branch pipe of tees: (a)A_2/A_1=0.8, (b)A_2/A_1=0.6

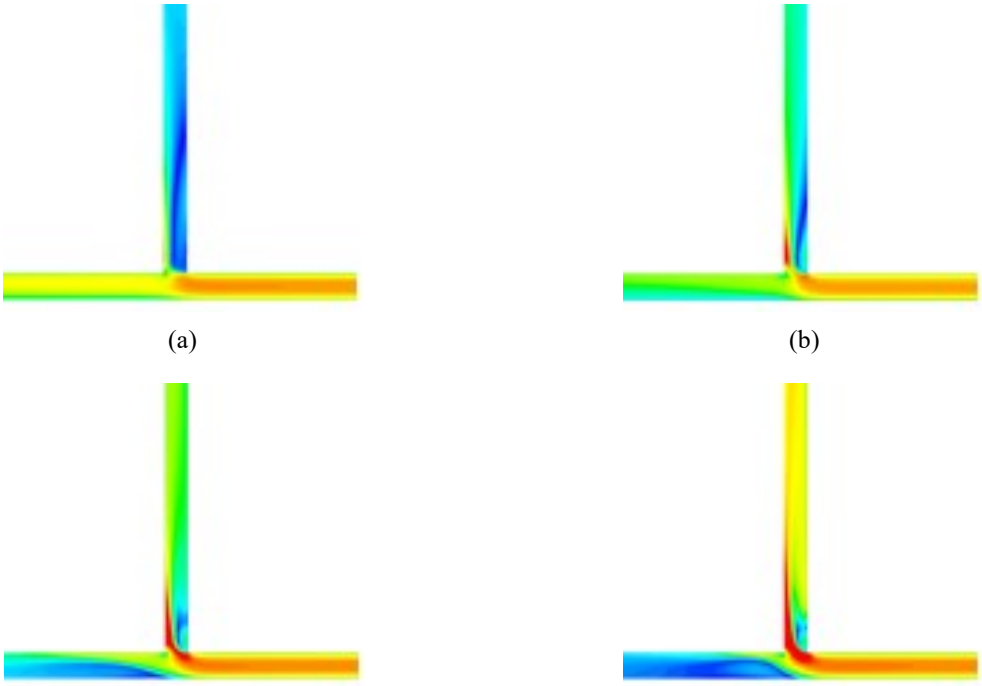

(a) (b)

(c) (d)

Figure 9: Contours of velocity magnitude: (a)Q_2/Q_1=0.2, (b)Q_2/Q_1=0.4, (c)Q_2/Q_1=0.6, (d)Q_2/Q_1=0.8

3.3 Minor Losses with respect to Area and Flow Rate Ratio

Figure 8(a) and (b) are distribution of minor losses at A_2/A_1 = 0.6 and 0.8, respectively. The solid line is Miller's chart, and dashed line marks the 10% range of error bounds. The present computation is overall shown less 10%. In Figure 4(b), no result exists on Miller's chart, so we can predict the minor losses only from the present results.

In Figure 8(a) and (b), the slope of K_{12} where $Q_2/Q_1 < 0.4$ becomes almost constant, but changes where $Q_2/Q_1 > 0.4$. The case of $Q_2/Q_1 > 0.4$ show that, as the flow ratio increases, the size of separation bubble generated in the branch shrinks by the forced suction from the branch(See Figure 9). This phenomenon attributes that as the inhaled flow increases, the flow is hindered by size of separation bubble, therefore, interacts with the flow by the size of separation bubble in the branch as the flow rate increased, and the flow velocity in the branch increases due to reduction of effective cross-sectional area from the continuity law. Therefore, the separation bubble suppresses the growth of separated vortex in the downstream due to the increased flow rate in the branch, and thus size of bubble is reduced, resulting in the abrupt change of the slope where $Q_2/Q_1 > 0.4$.

4. APPLICATION: 1-D SIMPLE NON-LOOP PIPE

4.1 Definition of Problem

Figure 9 is simple non-loop system for verification of the present hybrid method of 1-D and 3-D solver. In this research, we used the KYPIPE as 1-D solver while ANSYS-CFX as 3-D solver. Figure 9 shows a schematic of simple non-loop pipe problem. The branded flow(L3) can be used by turbomachinery such as pumps controlled by gate valves. The basic input data for 1-D code are supplied from the computation of 3-D code.

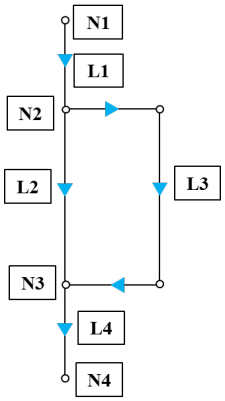

Figure 9: Schematic of simple non-loop pipe

4.2 Comparison of Results: Theory, 1-D Solver, and 3-D Solver

Table 3 shows the flow rate and pressure for each result, coinciding with each other. From this result, It was verified that the pipe system can be calculated without a 3-D Solver because the flow rate and pressure corresponding to each node(N_i) and line(L_i) can be predicted by simply specifying the minor losses. However, since 1-D solver could not show the detailed flow characteristics from the limitation of physical model, a 3-D solver should be required for the parts of plumbing such as 90-degree bends and T-junction branches. Depending on the numerical case, these should be used interchangeably.

Table 3: Result of the flor rate and pressure with theory, 1-D Solver, and 3-D Solver

Flow rate [m^3/s]			
	Theory	**1-D Solver**	**3-D Solver**
L1	0.0102	0.0102	0.0102
L2	0.0058	0.0057	0.0060
L3	0.0044	0.0045	0.0042
L4	0.0102	0.0102	0.0102

Pressure [kPa]			
	Theory	**1-D Solver**	**3-D Solver**
N1	112.048	111.863	111.669
N2	107.555	107.376	107.325
N3	105.936	105.812	106.056
N4	101.325	101.325	101.325

5. CONCLUSION

In this paper, we conducted the numerical simulation of bend-pipe and T-junction for Reynolds number between 100,000 ~ 10,000,000, and the following conclusions were obtained:

(1) In the bend pipe, without consideration of the wall roughness, the present result under-estimates the empirical correlation by Ito, (1960) for the minor loss of 90-degree bended pipes.

(2) The minor losses based on entrance to branch direction was less than 10% error compared to the Miller's chart, and It showed the similar trend regardless of the Reynolds numbers.

(3) In the Miller's chart, the new data of minor losses where $Q_2/Q_1 = 0.2$ and 0.4 and area ratio 0.8 were not presented, but we computed the data for the hidden region.

(4) Based on $Q_2/Q_1 = 0.4$ as criteria, the slope of minor loss changes in modes, which is the interaction effect of the separation bubble size and continuity law.

In additional, this paper only simulated the area ratio of 0.6 and 0.8 of T-junction. To simplify the three-dimensional simulation, a hybrid one-dimensional simulation is proposed, using the minor losses with geometrical and physical

ratios obtained from 3-D code, and the more complicated problems should be considered, which will be applied to the real systems of pipeline as a future work.

REFERENCES

Abdulwahhab, M., Injeti, N. K., & Dakhil, S. F. (2013). Numerical prediction of pressure loss of fluid in a T-junction. *Int. J. Energy Environ., 4*(3), 253-264.

Ayala, M., & Cimbala, J. M. (2020). Numerical approach for prediction of turbulent flow resistance coefficient of 90° pipe bends. *Proc. Inst. Mech. Eng. Part E: J. Process Mech. Eng. 0*(0), 1-10.

Badar, A. W., Buchholz, R., Lou, Y., & Ziegler, F. (2012). CFD based analysis of flow distribution in a coaxial vacuum tube solar collector with laminar flow conditions. *Int. J. Energy Environ. 3*(24), 1-15.

Boldy, A. P., (1970). *Performance of dividing and combining tees*, BHRA Tech. Rpt. 1061.

Costa, N. P., Maia, R., Proenca, N., & Pinho, F. T., (2006). Edge effect on the flow characteristics in a 90 deg tee junction. *J. Fluids Eng., 128*(6), 1204-1217.

Csizmadia, P., & Hös C., (2014). CFD-based estimation and experiments on the loss coefficient for Bingham and power-law fluids through diffusers and elbows. Comput. Fluids. 99(22), 116-123.

Gardel, A., (1957) Les pertes de charge daus les écoulements au travers de brachnements en té. *Bullentin Technique de la Suisse Romande, 9*(4), 123-130.

Ito H, (1960). Pressure losses in smooth pipe bend, J. Basic Eng. 82(1), 131-140.

Ito H, & Imai K., (1973). Energy losses at 90 deg pipe junction. *Proceedings of ASCE. (99 HY9) J. Hyd. Div.*

Kwon, H.J., Kim, M.H., Yun, Y.J., Chang, S.M., Cho, Y., (2021). Prediction of stability length and minor losses for the T-shaped bifurcated pipe with varying geometrical/physical ratios in the fully developed turbulent flow regime. *J. Comput. Fluids Eng.* 26(4), 83-90.

Maia, R. J., (1992). *Numerical and experimental investigations of the effect of local losses in piping systems methods and techniques for its systematic investigation. The specific case of the flow in a 90 deg tee junction*. Ph.D Thesis, University of Porto, Portugal.

Menon, E. S., (2015). Transmission pipeline calculations and simulations manual (1st Eds.). *Gulf Professional Publishing* (149-234), USA.

Miller, D. S., (1986) *Internal flow systems*, BHRA Fluid Engineering, Cranfield, UK.

Oka, K., & Ito, H., Energy losses at tees with large area ratios, *J. Fluid. Eng. 127*(1), 110-116.

Oka, K., Nozaki, H., & Ito, H., Energy losses due to combining of flow at tees, *JSME Int. J. Ser. B, 39*(3) 489-498.

Versteeg, H., & Malalassekera, W., (2007). *An introduction to computational fluid dynamics: the finite volume methods, 2nd-Eds*. UK: Pearson Education Limited.

White, F. M., (2016). *Fluid mechanics 8th-Eds.* New York, USA: McGraw-Hill Education.

Zhang, X., & Wang, Z., (2019). Assessment of hydraulic network models in predicting revers flow in OD cooled disc type transformer windings, *IEEE Access, 7*, 139249-139257.

ACKNOWLEDGEMENT

This study was supported by Korea Institute of Energy Technology Evaluation and Planning (KETEP, No.20208901000010). This paper is an extended version from the recent publication: Kwon et al. (2021).